

New insights into the mechanism of rehydration of milk protein concentrate powders determined by Broadband Acoustic Resonance Dissolution Spectroscopy (BARDS)

Vos, Bastiaan; Crowley, Shane V.; O'sullivan, Jonathan; Evans-hurson, Rachel; Mcsweeney, Seán; Krüse, Jacob; Ahmed, M. Rizwan; Fitzpatrick, Dara; O'mahony, James A.

DOI:

[10.1016/j.foodhyd.2016.04.031](https://doi.org/10.1016/j.foodhyd.2016.04.031)

License:

Creative Commons: Attribution-NonCommercial-NoDerivs (CC BY-NC-ND)

Document Version

Peer reviewed version

Citation for published version (Harvard):

Vos, B, Crowley, SV, O'sullivan, J, Evans-hurson, R, Mcsweeney, S, Krüse, J, Ahmed, MR, Fitzpatrick, D & O'mahony, JA 2016, 'New insights into the mechanism of rehydration of milk protein concentrate powders determined by Broadband Acoustic Resonance Dissolution Spectroscopy (BARDS)', *Food Hydrocolloids*.
<https://doi.org/10.1016/j.foodhyd.2016.04.031>

[Link to publication on Research at Birmingham portal](#)

General rights

Unless a licence is specified above, all rights (including copyright and moral rights) in this document are retained by the authors and/or the copyright holders. The express permission of the copyright holder must be obtained for any use of this material other than for purposes permitted by law.

- Users may freely distribute the URL that is used to identify this publication.
- Users may download and/or print one copy of the publication from the University of Birmingham research portal for the purpose of private study or non-commercial research.
- User may use extracts from the document in line with the concept of 'fair dealing' under the Copyright, Designs and Patents Act 1988 (?)
- Users may not further distribute the material nor use it for the purposes of commercial gain.

Where a licence is displayed above, please note the terms and conditions of the licence govern your use of this document.

When citing, please reference the published version.

Take down policy

While the University of Birmingham exercises care and attention in making items available there are rare occasions when an item has been uploaded in error or has been deemed to be commercially or otherwise sensitive.

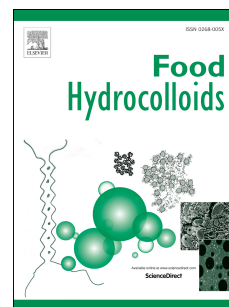
If you believe that this is the case for this document, please contact UBIRA@lists.bham.ac.uk providing details and we will remove access to the work immediately and investigate.

Download date: 05. May. 2023

Accepted Manuscript

New insights into the mechanism of rehydration of milk protein concentrate powders determined by Broadband Acoustic Resonance Dissolution Spectroscopy (BARDS)

Bastiaan Vos, Shane V. Crowley, Jonathan O'Sullivan, Rachel Evans-Hurson, Seán McSweeney, Jacob Krüse, M. Rizwan Ahmed, Dara Fitzpatrick, James A. O'Mahony



PII: S0268-005X(16)30167-9

DOI: [10.1016/j.foodhyd.2016.04.031](https://doi.org/10.1016/j.foodhyd.2016.04.031)

Reference: FOOHYD 3396

To appear in: *Food Hydrocolloids*

Received Date: 24 February 2015

Revised Date: 29 March 2016

Accepted Date: 20 April 2016

Please cite this article as: Vos, B., Crowley, S.V., O'Sullivan, J., Evans-Hurson, R., McSweeney, S., Krüse, J., Ahmed, M.R., Fitzpatrick, D., O'Mahony, J.A., New insights into the mechanism of rehydration of milk protein concentrate powders determined by Broadband Acoustic Resonance Dissolution Spectroscopy (BARDS), *Food Hydrocolloids* (2016), doi: 10.1016/j.foodhyd.2016.04.031.

This is a PDF file of an unedited manuscript that has been accepted for publication. As a service to our customers we are providing this early version of the manuscript. The manuscript will undergo copyediting, typesetting, and review of the resulting proof before it is published in its final form. Please note that during the production process errors may be discovered which could affect the content, and all legal disclaimers that apply to the journal pertain.

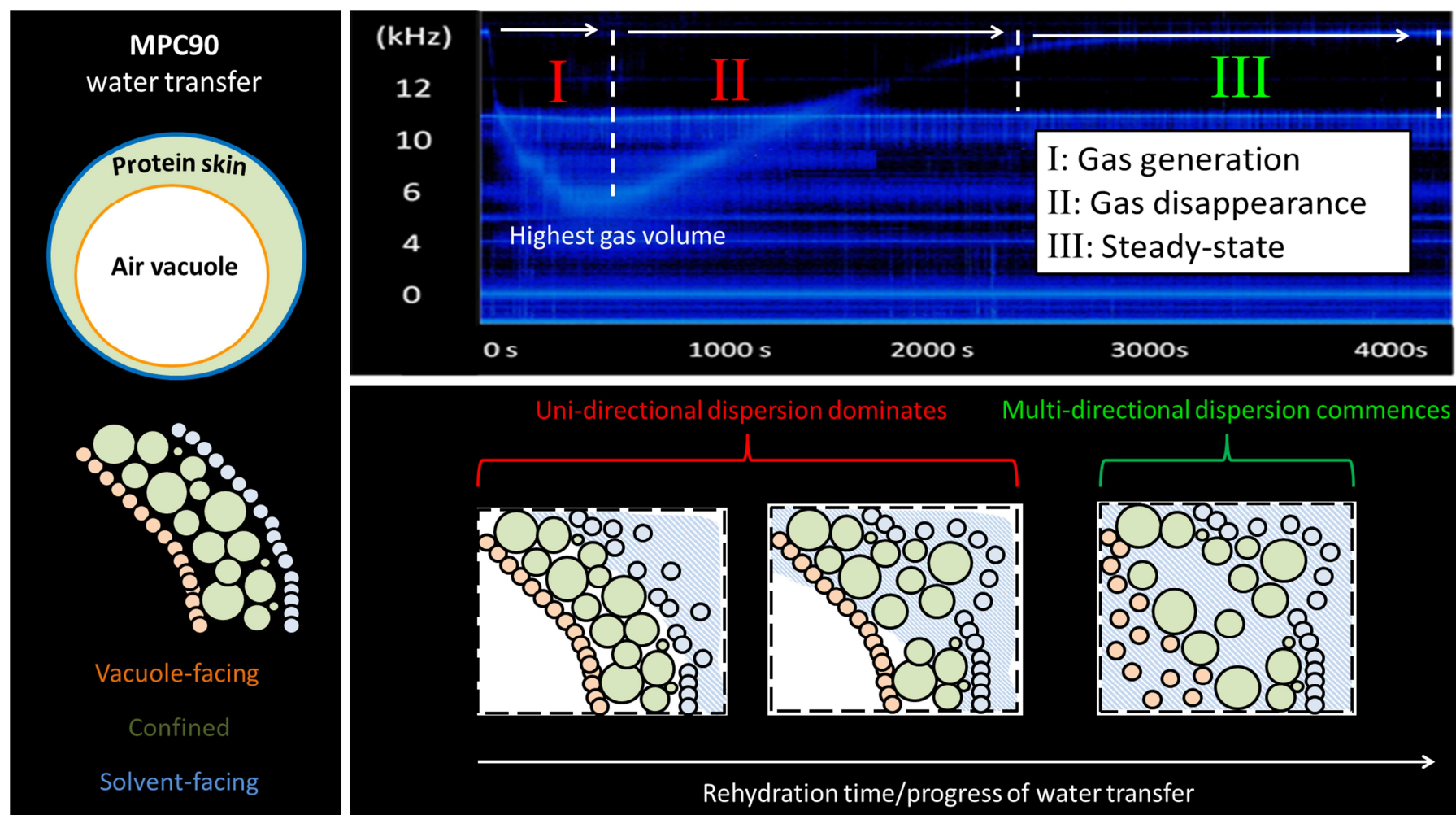


Figure 10.

**New insights into the mechanism of rehydration of milk protein
concentrate powders determined by Broadband Acoustic
Resonance Dissolution Spectroscopy (BARDS)**

Bastiaan Vos ^a, Shane V. Crowley ^b, Jonathan O'Sullivan ^{b,c}, Rachel Evans-
Hurson ^a, Seán McSweeney ^a, Jacob Krüse ^d, M. Rizwan Ahmed ^a, Dara
Fitzpatrick ^{a,*}, James A. O'Mahony ^b.

^a Department of Chemistry, Analytical and Biological Chemistry Research Facility
(ABCRF), University College Cork, Cork, Ireland.

^b School of Food and Nutritional Sciences, University College Cork, Cork, Ireland.

^c School of Chemical Engineering, University of Birmingham, Edgbaston, Birmingham, B15
2TT, UK

^d Kinetox, Beilen, The Netherlands.

* Corresponding Author: email address; d.fitzpatrick@ucc.ie

Abstract

This study investigated the transfer of water into milk protein concentrate (MPC) powder particles using Broadband Acoustic Resonance Dissolution Spectroscopy (BARDS) as a detection method for the first time. BARDS analysis is based on an acoustic phenomenon which occurs during powder rehydration. Release of air from the powder into the solvent during rehydration leads to outgassing in the solvent, which results in changes in solvent compressibility that are monitored through accompanying changes in induced resonance frequencies in the dissolution vessel. BARDS confirmed that water transfer into MPC particles became increasingly inhibited as protein content of the powder increased. The reproducibility of the data indicates that air release from internal vacuoles within powder particles in high-protein MPCs is a highly ordered process, occurring over a protracted time scale. Kinetic modelling of gas volume data from BARDS confirmed that the release of occluded air caused the changes in solvent compressibility during rehydration. The physicochemical properties of solubilised protein had a slight inhibitory effect on escape of bubbles from the solvent, but the primary factor limiting gas release from high-protein MPCs was water transfer into powder particles and the concomitant release of occluded air into the solvent. In agreement with many previous studies, cryo-SEM analysis showed that particles in high-protein MPCs were slow to disperse; the current study, in addition, highlights inhibited water transfer into particles as another factor which may contribute to their poor rehydration properties. A potential link between inhibited water transfer and poor dispersibility is proposed.

Keywords: MPC, BARDS, rehydration, solubility, water transfer, particle structure

1. Introduction

Milk protein concentrate (MPC) powders are recently developed ingredients which contain the two major protein fractions of bovine milk at the ratio that they occur naturally in milk (80:20 casein:whey protein). MPCs are typically manufactured using pressure-driven membrane separation processes, where ultrafiltration (UF) alone, or a combined UF and diafiltration (DF) process, is used to concentrate protein while removing smaller molecules including lactose, salts, non-protein nitrogen (Carr and Golding, 2016). After membrane processing, MPCs are usually spray-dried into powders. Currently, the most widely used MPC powders in commercial applications are the high-protein varieties (i.e., those containing $\geq 80\%$ protein). High-protein MPCs are exploited for their functional attributes (e.g., viscosity, emulsification, curd-forming ability) and nutritional features (e.g., high protein, low lactose) in a range of commercial applications (Agarwal *et al.*, 2015).

When milk protein concentrate (MPC) powders are manufactured to a final protein content $\geq 70\%$, solubility is commonly impaired (Crowley *et al.*, 2015), with the rate of liberation of casein micelles from powder particles during rehydration reducing with increasing protein content of the powders (Mimouni *et al.*, 2010b). As casein is the predominant component in high-protein MPCs, and the majority of caseins exist in the micellar state, the persistence of these poorly-dispersible particles for extended periods after wetting and submersion of the powder can result in suspensions with an unacceptably high quantity of sedimentable solids (Havea, 2006; Sikand *et al.*, 2011). Furthermore, after extended rehydration, these particles may not be of sufficient density to sediment, but may still remain suspended as large, highly-hydrated particles (Fang *et al.*, 2011; Crowley *et al.*, 2015). Incomplete rehydration of MPCs is an issue which is encountered both during mixing of dried ingredients by processors and reconstitution of dried products by consumers, and can have a negative influence on the functional and sensory properties of the final product (Carr and Golding, 2016).

Micellar casein is primarily responsible for the solubility issues encountered during the rehydration of MPCs (McKenna, 2000; Anema, 2006; Havea, 2006; Mimouni *et al.*, 2010a; Gazi and Huppertz, 2014). The particular solubility issues associated with MPCs are not found in whey protein-dominant powders (i.e., whey protein concentrates/isolates), casein-dominant powders which are relatively low in protein (i.e., skim milk/nonfat dry milk powders) or high-protein casein-dominant powders which do not contain micellar casein (e.g., sodium caseinate). Micellar casein concentrates (MCCs), powders with higher

casein:whey protein ratios than MPCs, are known to have similarly poor, and even more challenging, rehydration performance (Crowley *et al.*, 2016); when levels of lactose or whey proteins are increased in MCCs they dissolve more quickly, due to a concurrent decrease in the level of micellar casein and possible improvements in the water transfer properties of the powder due to the presence of the more soluble components (Richard *et al.*, 2012).

In high-protein MPC powders, casein micelles are considered to be the molecular building blocks of a 'skin' at the surface of primary powder particles, which may prevent the release of casein micelles during rehydration (McKenna, 2000; Mimouni *et al.*, 2010b; Fyfe *et al.*, 2011; Crowley *et al.*, 2016; Ji *et al.*, 2016). The solubility of MPCs deteriorates further during storage under adverse conditions (Anema *et al.*, 2006; Fyfe *et al.*, 2011; Gazi and Huppertz, 2014), due to the decreased solubility of micellar casein, while the solubility of whey proteins is largely retained unless they have been denatured to a significant degree during processing (Gazi and Huppertz, 2014). The central role of micellar casein in the development of insolubility issues in MPCs is further supported by some of the techniques which have been used to improve their solubility, including high pressure treatment (Udabage *et al.*, 2012), ion-exchange (Bhaskar *et al.*, 2001) and CO₂ injection (Marella *et al.*, 2015), all of which are primarily based on structural modification of casein micelles (Carr and Golding, 2016).

There is a need to develop *in-situ* techniques for the dynamic monitoring of powder rehydration phenomena, as this will allow the identification of the stages (i.e., wetting, water transfer, or dispersion) which are responsible for prolonged rehydration times (Fang *et al.*, 2008; Crowley *et al.*, 2016). Dynamic studies of MPC powder rehydration have primarily focused on advanced stages of rehydration, such as dispersion, which has been identified as the rate-limiting step in the rehydration process for MPCs in experiments where the changes in particle size over time were measured (Mimouni *et al.*, 2009; Fang *et al.*, 2011). However, other than the study of Hauser and Amamcharla (2016) on commercial MPC80, there are limited studies available in the literature in which water transfer into particles during the rehydration of different MPC powders has been investigated. Water transfer has been studied in MCCs by Schuck *et al.* (2002) and Richard *et al.* (2012) using nuclear magnetic resonance relaxometry and ultrasound attenuation measurements, respectively, with both studies demonstrating that water transfer can be markedly inhibited in MCCs. Bouvier *et al.* (2013) demonstrated that increasing the size and number of pores in particles can improve the rehydration properties of MCC powders, supporting the concept that enhancing water transfer can improve the dispersibility of these powders.

Generating data on water transfer phenomena in MPCs could potentially inform strategies to modify particle structure (i.e., during or after spray drying) in order to improve their rehydration characteristics. Thus, in this study, a new form of acoustic spectroscopy, Broadband Acoustic Resonance Dissolution Spectroscopy (BARDS), was used to monitor water transfer related phenomena in a range of MPC powders for the first time. BARDS is an analytical platform technology with multiple applications, such as blend uniformity analysis, discrimination of polymorphs and drug loading on sugar spheres for controlled release formulations (Fitzpatrick *et al.*, 2012a, 2012b, 2014).). The technique is based on real-time changes in the compressibility of a solvent as a solute dissolves, which can be monitored acoustically via changes in induced resonant frequencies of the dissolution vessel. In this study, the rehydration behaviour of MPCs with varying protein contents was assessed over time using BARDS. Experiments were devised to isolate the influence of water transfer on changes in gas volume during rehydration. A novel kinetic approach was used to confirm the role of occluded air release in determining BARDS spectra. The influence of serum-phase composition (i.e., soluble protein) on the escape of gas from the solvent was considered for the first time in a study of dairy powder rehydration based on changes in gas volume. Cryo-SEM micrographs were also collected during the rehydration of selected powders to establish a potential link between water transfer and particle dispersion-state.

2. Experimental

2.1. Materials

Crowley *et al.* (2014a, b) described the manufacturing protocol for pilot-scale production of the MPC powders used in the current study. In brief, pasteurised skim milk was subject to UF (MPC50, MPC60) or UF and DF (MPC70, MPC80, MPC85, MPC90) to different protein concentration factors at 50°C with 10 kDa molecular weight cut-off membranes. MPC35 did not undergo any membrane filtration, and is essentially skim milk powder. MPC35, MPC50, MPC60 and MPC70 were evaporated before being spray-dried, while MPC80, MPC85 and MPC90 were not subjected to evaporation. Spray drying involved nozzle atomisation, an air inlet temperature of 185-190°C and an outlet temperature of 85-90°C. The composition and selected physical properties (measured as described by Crowley *et al.* (2014a, b) of the MPC powders is provided in Table 1. Analar grade KCl was purchased from Sigma Aldrich. The solvent used for rehydration experiments was deionised water unless otherwise indicated.

[Table 1 about here]

2.2. Instrumentation

The BARDS spectrometer consists of a closed chamber with a dissolution vessel (soda lime glass), microphone (Sony ECM-CS10, range 100 Hz – 16 kHz), a magnetic stirrer and follower. A schematic diagram is shown in Figure 1, demonstrating the principle of BARDS as applied in the current study and the basic components of the apparatus. There is access at the front of the chamber for the dissolution vessel and at the top in order to place a sample in a weighing boat on an automated tipper motor for introduction of the powder. The microphone is positioned above the top of the glass within the housing for these studies. The glass, containing 25 mL of deionised water, is placed on the stirrer plate. The stirrer motor underneath is positioned so as to allow the magnetic follower to gently tap the inner vessel wall. In this way, the follower acts as a source of broadband acoustic excitation, thereby inducing various acoustic resonances in the glass, the liquid and the air column above the liquid. The audio is sampled at a rate of 44.1 kHz. A fast Fourier transform is applied to the signal, resulting in a typical BARDS frequency response. The resonances of the liquid vessel are recorded in a frequency band of 0-20 kHz. The frequency response was measured during the rehydration of 0.04-0.20% (w/v) suspensions of MPCs in 25 mL water.

[Figure 1 about here]

2.2.1 Theoretical Background of BARDS

The BARDS response results from changes in the compressibility of a solvent during the dissolution of a compound, in which compressible gas bubbles are introduced or generated. Changes in compressibility alter the speed of sound resulting in frequency changes of induced acoustic resonances within the solvent. The principles underlying the BARDS response are as follows. The sound velocity (v) in a medium (m s^{-1}), whether air or liquid phase, is determined by Equation 1.

$$v_{(\text{sound})} = \sqrt{\frac{1}{K \cdot \rho}} \quad \text{Equation (1)}$$

Where ρ is the density (kg m^{-3}) and K is the compressibility (inverse of the bulk modulus) of the medium (Pa^{-1}). Generation of micro bubbles in a liquid decreases the density in a negligible way in comparison to a large increase in compressibility. The net effect is a significant reduction of the sound velocity in the liquid. The following relationship between the fractional bubble volume and the sound velocity in water was derived by Frank S. Crawford, as given in equation 2 (Crawford, 1982):

$$\frac{v_w}{v} = \sqrt{(1 + 1.49 \times 10^4 \cdot f_a)} \quad \text{Equation (2)}$$

where v_w and v are the velocities of sound (m s^{-1}) in pure and bubble-filled water, respectively, and f_a is the fractional volume occupied by air bubbles. Equation 2 is based on an approximation presented originally by Wood (1930).

BARDS analysis of an induced acoustic excitation of the vessel containing the fluid is focused on the lowest variable frequency time-course, i.e., the fundamental resonance mode of the liquid. The fundamental resonant frequency is determined by the sound velocity in the liquid and the approximate but fixed height of the liquid level, which corresponds to one quarter of its wavelength. The frequency response is described as:

$$freq = \frac{freq_w}{\sqrt{1 + 1.49 \times 10^4 \cdot f_a}} \quad \text{Equation (3)}$$

where $freq_w$ and $freq$ are the resonance frequencies (kHz) of the fundamental resonance modes in pure and bubble-filled water, respectively. A comprehensive outline of the principles and underlying processes involved in BARDS analysis is given by Fitzpatrick *et al* (2012a).

2.3. Experimental procedure for BARDS experiments

In a typical experiment, the spectrometer records the steady-state resonances of the system as a reference for 30 s after the stirrer has been set in motion (Figure 1, panel 1). The pitch of the resonance modes in the solution change significantly when the powder is added (Figure 1, panel 2), before gradually returning to steady-state over several minutes (Figure 1, spectrum in panel 3). The amounts used are expressed as solid/liquid concentration (w/v) in all figures and throughout the text. Gas oversaturation of water prior to introduction of powders was removed through agitation by shaking vigorously for 60 s and then resting for

10 min. Otherwise, remaining gas oversaturation may lead to an over-response (Fitzpatrick *et al.* 2013).

The frequency-time response of the fundamental resonance is presented as manually extracted data from the total acoustic response. The steady-state frequency before addition of the powder is designated as the 'volume line', so called as it varies depending on the liquid volume in the vessel. Spectra were recorded for 3000-4000 s depending on the rate of return of the BARDS response to steady state. All experiments were performed in duplicate at ambient temperature (~22°C) and atmospheric pressure. Average readings with error bars representing the standard deviation are presented.

2.4. Characterisation of the microstructure of MPC powders in their dry state

Scanning electron microscopy (SEM; Philips XL30 FEG ESEM) was used to characterise the microstructure of MPC35, MPC70 and MPC90 to assess any morphological differences. MPC powder samples were placed upon double-sided adhesive conductive carbon tape, sputter-coated with gold and scanned at 10 kV.

2.5. Characterisation of the microstructure of MPC powders during rehydration

Cryogenic scanning electron microscopy (Cryo-SEM; Philips XL30 FEG ESEM), with a Gatan low temperature preparation system, was used to visualise the microstructure of MPC35 and MPC90 at rehydration times of 100, 1000 and 3000 s. Cryo-SEM analysis was performed to assess differences in particle dispersion between the two powders, to supplement water transfer data generated using BARDS. One drop of liquid was frozen to approximately -180 °C in liquid nitrogen slush. Samples were then fractured and etched for 1 min at a temperature of -95 °C inside the preparation chamber. Afterwards, samples were sputter coated with gold and scanned at 3 kV, during which the temperature was maintained below -160 °C by addition of liquid nitrogen to the system.

3. Results

3.1 Composition and physical properties of the MPC powders

Data related to the composition and physical properties of the MPCs are shown in Table 1. Reductions in lactose and mineral levels were measured in the MPC powders, corresponding with increasing protein concentration. Particle size increased with increasing protein content for MPC35, MPC50 and MPC60, and decreased thereafter as protein content increased further. There were no apparent trends in the volume of interstitial and occluded air when MPC35, MPC50, MPC60 and MPC70 were compared; however, MPC80, MPC85 and MPC90 were 2-3 times more aerated than the former powders, although there were only minor differences within this class of high-protein MPC powders.

3.2 Interpretation of BARDS profiles

Figure 1, panel 3, shows a typical BARDS spectrum during the rehydration of MPC90. The acoustic frequency profile of interest is called the fundamental curve. The frequency minimum (f_{min}) represents an equilibrium between the rate of introduction of gas as bubbles into solution and the rate of elimination of these bubbles at the surface of the solution. In BARDS analysis, the fundamental curve is used to make comparisons between individual experiments. The acoustic frequencies of the vessel remained steady for the first 30 s until the addition of MPC90; thereafter, the resonant frequency at 14 kHz decreased to 6 kHz and gradually returned to steady-state. The constant frequency at 11 kHz is just one of many resonant frequencies of the vessel that is not dependent on the liquid compressibility and therefore remained unchanged as gas volume levels fluctuated.

Figures 2 and 3 show the acoustic profiles for all seven MPCs with a concentration of 0.2%. There is a gradual increase in the deflection to f_{min} with increasing protein content. Powders with higher protein concentrations exhibited a distinct change in the rate of gas release into the solvent (reduced down-slope) compared to lower protein powders, as indicated by the increased amount of time required to reach f_{min} . The disappearance of gas from the solvent after f_{min} also proceeded more slowly (reduced up-slope) as protein content of the MPC powder increased, which resulted in considerably extended times to reach steady-state. Most notable was the time required (~3000 s) to reach steady-state for MPC90.

[Figure 2 about here]

The acoustic profiles (Figure 2) strongly indicate differences in the volume of gas generated, the rate of gas release from the powders, and the rate of gas disappearance from the solvent during the rehydration of different MPCs. These factors were investigated more closely by tracking changes in gas volume in the following sections.

3.3 Changes in compressible gas volume during rehydration of MPC powders

Equation 3 was applied to the BARDS frequency data from the MPC experiments (Figure 2) to generate data relating to the fractional gas volume (f_a) occupied by compressible gas during the dissolution of 0.2% of each of the MPCs. The gas volume plots presented in Figures 3 (A) and (B) concern absolute volumes ($f_a \times V_{\text{solution}}$). The initial up-slope indicates the rate at which gas was released from the powder. The data suggests that a significant change in rehydration behaviour occurred when the protein content exceeded 80% in the MPC powders. MPC35 generated a negligible gas volume during rehydration (see higher resolution data in Figure 3, B). MPC50 and MPC60 exhibited a very rapid release of a limited quantity of gas, the disappearance of which from the solvent began immediately and proceeded rapidly. Conversely, for MPC80, MPC85 and MPC90, there was a very gradual increase in the gas volume to a high maximum, after which point gas remained constant in the system for ~200 s, due to a balance of gas release and disappearance, before gas disappearance from the liquid surface became dominant. The steady increase in the compressibility of the solvent for these powders during ~ 500 s of rehydration indicates that the immersed particles themselves, containing occluded air prior to significant water transfer, are non-compressible and that, as such, the release of gas from the particles contributes to changes in the compressibility of the solution. If the particles themselves were compressible, an immediate and marked increase in gas volume would be expected to occur as soon as the powder submerged.

[Figure 3 about here]

3.4 Kinetic analysis of changes in compressible gas volume during rehydration of the MPCs

When the gas volume data (Fig. 3 A, B) is plotted using a logarithmic scale, as shown in Figure 3 (C), the disappearance rate constant (k) for compressible gas in the solution is given by the descending slope (assuming a first-order process). Table 2 presents the results of this gas disappearance analysis, with values for k and the time range from which the descending slope was calculated. For the MPC suspensions at the highest concentration studied (0.2%), a gradual decrease in gas disappearance rate is observed with increasing protein content of the powder. The k value of the lowest protein powder (MPC35) was five times that of the highest protein powder (MPC90), indicating a profound shift in water transfer behaviour.

[Table 2 about here]

Based on visual assessment of wetting behaviour, kinetic data in Table 2 and gas volume-time plots (Fig. 3), it is possible to distinguish four categories of MPC based on data for 0.2% systems:

Fast wetting/fast water transfer/fast gas disappearance: MPC35 and MPC50

These powders wetted rapidly at the water surface and underwent fast sinking. The volume response-time curves for these samples show a subsequent fast release of compressible gas from the powder into the solvent, indicating that water transfer into particles was rapid after sinking. In contrast to the MPC50, the MPC35 response seems to indicate a relatively slower rate of water transfer, despite having a lower protein content. Both powders exhibited high gas disappearance rates ($k \approx 1-3 \times 10^{-2} \text{ s}^{-1}$) compared to the other MPCs. These results are generally in line with previous studies demonstrating that low-protein MPCs have good solubility characteristics (Crowley *et al.*, 2015; Sikand *et al.*, 2011)

Fast wetting/fast water transfer/intermediate gas disappearance: MPC60 and MPC70

These samples exhibited rapid wetting at the powder surface and gas generation in the solvent, suggesting that water transfer into particles in these powders was not severely inhibited compared to MPC35 and MPC50. Like MPC50, these powders exhibited a more rapid rate of water transfer than MPC35. However, both powders exhibit slower gas disappearance rates ($k \approx 3.7\text{--}6.6 \times 10^{-3} \text{ s}^{-1}$) than MPC35 and MPC50, indicating that escape of bubbles from the solvent was inhibited compared to the lower protein powders, likely due to the increasing influence of solubilised protein. For example, a 0.2% solution of MPC70 will have approximately double the protein content of MPC35. Particles in this set of MPCs with <80% protein disperse relatively quickly (Crowley *et al.*, 2015), and therefore increasing the protein content from MPC35/MPC50 to MPC60/MPC70 may have increased the levels of soluble protein to a degree sufficient to inhibit bubble escape (Ybert and di Meaglio, 1998).

Slow wetting/slow water transfer/intermediate gas disappearance: MPC80 and MPC85

The initial part of the response was likely influenced by slow wetting, with MPC80 and MPC85 observed to require ~200 s to fully disappear from the liquid surface; however, this cannot account for the 500 s of gas generation which elapsed prior to the initiation of the gas disappearance phase, which was strongly indicative of inhibited water transfer into powder particles. As with MPC60 and MPC70, intermediate gas disappearance rates ($k \approx 3.4 - 3.9 \times 10^{-3} \text{ s}^{-1}$) were measured, which suggests that the period of inhibited water transfer did not continue into the gas disappearance phase and influence derived k values. Thus, the effect of soluble proteins might be considered to dominate gas disappearance, as per the lower protein MPCs.

Slow wetting/slow water transfer/slow gas disappearance: MPC90

Similarly to MPC80 and MPC85, slow wetting was observed for MPC90 (~200 s). The initial part of the response of MPC90 is also similar to that of MPC80 and MPC85, and strongly

indicates inhibited water transfer into the submerged particles. The gas disappearance rate for MPC90 was the lowest of all the powders ($k \approx 1.9 \times 10^{-3} \text{ s}^{-1}$), and suggested that water transfer may have continued during the gas disappearance phase.

The slow gas generation for high-protein MPCs strongly indicates inhibition of water transfer into powder particles. However, it is not clear, especially for MPC90, which of the two primary phenomena (water transfer into particles and gas elimination from the solvent) are rate-determining for the observed trends in gas disappearance based on the kinetic data for 0.2% systems alone. Further analysis of the concentration-dependency of the BARDS response for different MPCs was performed to obtain more reliable mechanistic and kinetic information.

The concentration-dependency of the BARDS response for four of the seven MPCs (MPC35, MPC70, MPC80 and MPC90), spanning the four aforementioned categories, is shown in Figure 4. The comparative kinetic analysis of the BARDS data is based on the related gas volume data and is presented in Figure 5 using a logarithmic scale.

[Figure 4 about here]

[Figure 5 about here]

The results for individual powders can be summarised as follows:

MPC35 (Figure 5, A):

An immediate, very rapid gas disappearance was observed for 0.04 and 0.08% systems ($k \approx 5 \times 10^{-2} \text{ s}^{-1}$). A short time period (~200 s) of constant gas volume was observed at the higher concentrations of 0.12% (~100 s) and 0.16 and 0.20% (~200 s) before the gas volume started to decrease. The periods of constant volume may be attributed to slower powder wetting and uptake into the solvent, which was observed with higher quantities of added MPC35. In the

gas disappearance phase, a k value of $\sim 1 \times 10^{-2} \text{ s}^{-1}$ was calculated for concentrations of 0.08 - 0.20%.

MPC70 (Figure 5, B):

The gas disappearance rate for the concentrations 0.04 – 0.16% decreased gradually with time. Therefore, the curves have been characterized by two gas disappearance rate constants, an initial fast release and a subsequent slow release: the values are $k \approx 1.2\text{-}1.7 \times 10^{-2} \text{ s}^{-1}$ for the initial part of each curve and $k \approx 7\text{-}8 \times 10^{-3} \text{ s}^{-1}$ for the terminal parts. The gas disappearance for the 0.2% system was much slower than these lower concentrations with $k \approx 6.6 \times 10^{-3} \text{ s}^{-1}$ for the initial part and $k \approx 3.7 \times 10^{-3} \text{ s}^{-1}$ for the terminal part of the curve. The overall decrease in disappearance rate with rehydration time and with increase of MPC70 concentration, may suggest an increasing influence of solvent properties (e.g., increasing viscosity or ‘protein drag force’ effects) on the release of bubbles from the solvent as protein is solubilised.

MPC80 (Figure 5, C):

The time taken for the gas volume to reach its maximum value increased with increasing concentration, due to the influence of increasingly longer wetting times (200 s at the highest mass added). The gas disappearance rate constants decreased with increasing concentration from $k \approx 6.7 \times 10^{-3} \text{ s}^{-1}$ at 0.04% to $k \approx 3.4 \times 10^{-3} \text{ s}^{-1}$ at 0.2%.

MPC90 (Figure 5, D):

Compared to MPC80, the concentration-dependency of the time for the gas volume to reach its maximum seemed less prominent with MPC90, despite this powder having similar wetting times. In addition, the gas disappearance rate appears to be relatively independent of concentration ($k \approx 2.0\text{-}3.0 \times 10^{-3} \text{ s}^{-1}$) compared to the other MPCs.

The rate-limiting stage for the descending slope (representing gas disappearance) seems to be gas elimination from the solvent MPC70. Values for k decrease with increasing concentration, indicating that increasing levels of solubilised components may have retarded bubble escape to a greater degree. On the other hand, for MPC90, gas release from MPC particles appears to be rate-limiting, as gas disappearance was effectively independent of concentration. A slow and ordered process of water transfer into MPC90 particles would explain this observation.

The MPC80 data indicate a concentration-dependent transition between the processes described which determine the gas disappearance rate for MPC70 and MPC90. Like MPC90, there is evidence that this powder has poor water transfer properties, due to the extended duration of its gas generation phase, but its gas disappearance behaviour is broadly similar to MPC70. It is proposed that the factor which extends the gas disappearance phase of MPC90 compared to MPC80 is a slower water transfer process.

3.6 Validation of water transfer as key stage influencing BARDS spectra for MPC90

The data presented in previous sections indicate that inhibited water transfer into particles in high-protein MPCs strongly influences the BARDS spectra, with powders such as MPC90 containing particles which require longer water transfer times. An experiment was designed to investigate whether the slow decrease in the compressible gas volume for high-protein MPC samples (especially MPC90) is due to steady transfer of gas out of the MPC particles (during water transfer) or due to other processes which affect the loss of gas at the liquid surface - for instance, an increase in viscosity, surface tension or drag forces acting on ascending bubbles (Ybert and di Meaglio, 1998). To this end, KCl was used as a monitoring compound, to investigate whether the physicochemical properties of rehydrated MPC90 (post steady-state) inhibited the ability of gas to escape from the liquid. Figure 6 (A) shows the BARDS responses during the dissolution of 0.5 M KCl in water and also the dissolution of 0.2% MPC90 in water. KCl exhibits immediate release of gas and a fast return to steady state within 200 s.

[Figure 6 about here]

A second experiment was performed whereby the same amount of KCl was added to a solution of 0.2% MPC90 which had been rehydrated until a steady-state BARDS response was achieved (Fig. 6, B). Again, there was an immediate generation of gas observed, but the return to steady-state took ~10 times longer due to replacement of water with MPC90 solution. This result shows that the presence of soluble proteins impedes gas disappearance. Despite the slower escape of gas from the liquid, it took a significantly shorter time for gas from KCl to disappear from MPC solution compared to the disappearance of gas during the rehydration of MPC90. The first-order k values can be derived from the descending slopes in Figure 6 (B), and were found to be $2.8 \times 10^{-3} \text{ s}^{-1}$ for KCl dissolved in MPC90 solution compared to the lower k value of $1.5 \times 10^{-3} \text{ s}^{-1}$ for MPC90 on its own. This strongly indicates that for MPC90 the terminal gas disappearance rate is determined by the process of continued water transfer into particles generates compressible gas from MPC90 during rehydration.

In pharmacokinetics, an analogous process to that observed for MPC90 rehydration can be described in which the terminal stage of the concentration time-course of a drug in the blood reflects the drug absorption process instead of the elimination process as a 'flip-flop' system (Boxenbaum, 1998). In this study, generation of compressible gas bubbles through water transfer into particles can replace absorption, in the pharmacokinetic sense, for the kinetic analysis of MPC90 rehydration presented in the following section.

3.7 Verification that occluded air accounted for total gas volume using flip-flop kinetics

The gas volume time-course of MPC90 (see Figure 3, A) was used to establish the total amount of compressible gas that was produced during the rehydration experiment. An approach was followed similar to that used in pharmacokinetic studies, in which one distinguishes the absorption of a drug into the body, its distribution and its subsequent elimination. The concentration-time profile is determined in the central compartment (blood/plasma). The area under the concentration/time curve (AUC), combined with the drug

distribution volume (V_d) and its first-order elimination rate constant (k_{el} , s^{-1}) are used to calculate the dose (D) that has entered the central compartment using equation 4.

$$D = AUC \times V_d \times k_{el} \quad \text{Equation (4)}$$

In an adjusted approach used for the gas volume analysis, the absorption is replaced by the generation of compressible gas into the solution (the central compartment) following addition of MPC90 to the solvent. The dose administered in pharmacokinetics becomes the total amount of compressible gas produced. In contrast to pharmacokinetics, the distribution volume (V_d) is now simply the volume of the solution ($V_{solution}$) (Rowland and Tozer, 1989). The total amount of compressible gas produced during dissolution (D_{gas}) can then be calculated using Equation 5.

$$D_{gas} = AUV \times k_{el} \quad \text{Equation (5)}$$

Where D_{gas} (mL) is the total amount of compressible gas produced during the rehydration of MPC90. AUV (mL.s) is the total area under the gas volume/time curve (the volume of compressible gas is calculated as $f_a \times V_{solution}$) and k_{el} (s^{-1}) is the rate constant of the first-order gas elimination process. In the calculations, the rate constant determined for KCl in MPC90 is used for the elimination process. The results of the modelling are shown in Figure 7. The red profile in Figure 7(A) represents 0.2% MPC90 and the black profile is the simulation with a k_{gen} (gas generation rate) of $1.54 \times 10^{-3} s^{-1}$, derived from MPC90 terminal gas disappearance rate and k_{el} (gas elimination rate) is $2.82 \times 10^{-3} s^{-1}$, derived from KCl gas elimination rate in MPC90 solution. Figure 7 (B) shows the log plot of the data in Figure 7 (A). The AUV was calculated to be 7.87 mL.s. The total amount of gas generated was 2.22×10^{-2} mL, calculated as $AUV \times k_{el}$; note that $k_{el} > k_{gen}$, implying flip-flop characteristics of gas production and elimination. The total amount of occluded gas in the MPC90 sample used in the experiment was 2.31×10^{-2} mL. This was estimated for a 0.2% MPC90 system in 25 mL of water from the occluded air value in Table 1. The total amount of gas generated during powder rehydration (estimated from BARDS data) is in very close agreement with the occluded air content of the powder.

[Figure 7 about here]

487

488 A similar set of experiments with rehydration of MPC90 in water and KCl in rehydrated
 489 MPC90, but performed under slightly altered conditions (i.e., using a glass vessel with
 490 different dimensions and therefore slightly different solution mixing dynamics) yielded
 491 different gas elimination rate constants. However, the total amount of compressible gas
 492 calculated was the same as found with the other experiment and again corresponded to the
 493 value for occluded gas in MPC90. The results of the experiment are shown in Figure 7 (C)
 494 and (D). The red profile in Figure 7 (C) represents 0.2% MPC90 and the black profile the
 495 simulation with k_{gen} of $1.99 \times 10^{-3} \text{ s}^{-1}$, derived from MPC90 terminal gas disappearance rate.
 496 The value for k_{el} of $5.17 \times 10^{-3} \text{ s}^{-1}$ was derived from the KCl gas elimination rate in MPC90
 497 solution. The AUV was calculated to be 4.36 mL.s and the total amount of gas generated was
 498 $2.25 \times 10^{-2} \text{ mL}$, calculated as $AUV \times k_{el}$; flip-flop characteristics are implied again as $k_{el} >$
 499 k_{gen} . The calculated total gas volume was in excellent agreement with the total amount of
 500 occluded gas in the MPC90 sample used in the experiment ($2.31 \times 10^{-2} \text{ mL}$). The
 501 calculations demonstrate that the two experiments are in good agreement in terms of the total
 502 amount of gas generated. The value is therefore independent of the differences in response
 503 observed between the two experiments and the different rate constants used in the
 504 calculations.

505 Crucially, the values calculated using flip-flop kinetics for the amount of gas
 506 generated during the rehydration of MPC90 indicate that the gas detected by BARDS
 507 originates exclusively from the occluded gas fraction of the powder. Thus, when considering
 508 the BARDS spectra for the MPC90, the influence of interstitial air can be considered
 509 negligible, which allows isolation of the gas generation phenomenon as one of water transfer
 510 into powder particles.

511

512

513 3. 8 Microstructure of dry MPC powders

514 SEM micrographs of representative low- (MPC35), intermediate- (MPC70) and high-
 515 protein (MPC90) powders are shown in Figure 8. In agreement with particle size data (Table
 516 1), there was a greater quantity of small particles in the MPC90, while the MPC35 and MPC70

were similar in this respect. Increasing protein content was associated with two distinct morphological changes, the smoothening of particle surfaces and partial deflation of the surface towards the particle interior. Smooth particle surfaces may be attributable to differences in compositional homogeneity of the particle surfaces in the MPC powders. Kelly *et al.* (2015) determined that protein constituted 63, 79 and 93% of the surface of MPC35, MPC70 and MPC90 (same sample set), respectively; the surface of MPC35 contained a large quantity of lactose (31%), while the surface of MPC90 contained <1% lactose. The deflation effect is characteristic of casein-dominant dairy powders, such as MPCs and MCCs, and is not observed for whey protein-dominant powders (Sadek *et al.*, 2016). It is generally associated with powders containing high levels of occluded air, which is the case for MPC70 and, in particular, MPC90 (Table 1), where distinct internal air vacuoles and external protein layers are present. Recent studies suggest that highly concentrated casein suspensions undergo a form of gelation during drying, and that this surface gel has distinct mechanical properties which result in this final deflated or buckled powder particle shape (Sadek *et al.*, 2016).

[Figure 7 about here]

3.9 Microstructure of MPC powders during rehydration

To investigate the dispersion state of powder particles during rehydration, cryo-SEM was used to visualise powders with fast (MPC35) and slow (MPC90) water transfer characteristics. Cryo-SEM micrographs of MPC35 and MPC90 powders during rehydration are shown in Figure 9. The three different time points represent pre-steady-state for both powders (100 s), steady state for MPC35 and not MPC90 (1000 s), and post-steady-state for both powders (3000 s), as determined by BARDS.

[Figure 9 about here]

After a short period of 100 s, partially-dispersed or fragmented particles were present in both MPC35 and MPC90; however, the latter also contained intact powder particles, similar in

size ($\sim 20\ \mu\text{m}$) to the particles observed in the corresponding micrographs for dry powders (Figure 8). When the powders were rehydrated for 1000 s, numerous small, distinct particles predominated in MPC35 which were $\sim 1\ \mu\text{m}$ in size, while several larger particles ($\sim 5\ \mu\text{m}$) remained in MPC90 with few distinct particles in general being visible. After 3000 s of rehydration, the majority of particles in MPC35 were $< 1\ \mu\text{m}$, with a minor distribution of micron-sized particles, while, in contrast, MPC90 was still populated largely by particles $> 1\ \mu\text{m}$; in addition, ring-link structures can be seen in Figure 9 (1C), consistent with the possible presence of hydrated but undispersed powder particles, as suggested previously (Mimouni *et al.*, 2009; Crowley *et al.*, 2015). Figure 9 also shows the BARDS frequency-time profiles for all seven MPCs with a sample mass of 50 mg (0.2%). The BARDS measurement times corresponding to the rehydration times where the micrographs were captured are indicated. It can be seen in Figure 9 that for an equivalent stage of water transfer, such as the steady-state of all MPCs at 3000 s, different dispersion states can exist. This is because BARDS is a technique that detects the completion of water transfer into particles but not necessarily the disappearance of granular particle structures. However, both water transfer and dispersion occur simultaneously, indicating that a possible relationship between the two phenomena exists; this is expanded in Section 4.

4. Discussion

This is the first study reporting on the gas release/water transfer properties of a full range of MPCs, ranging from low to high protein. Results from BARDS analysis indicated that water transfer into MPC powder particles became inhibited as the protein content of the MPC powders increased (Figures 2, 3, Table 1). For example, rehydration of MPC35 yielded a minimal BARDS response and a rapid return to steady-state ($< 400\ \text{s}$), while the time (60 min) required to reach steady-state for MPC90 (0.2%) (Figure 2) is unprecedented in its length compared to previous BARDS studies (Fitzpatrick *et al.*, 2012a, 2012b, 2013, 2014). Release of gas from powders can be used to indirectly investigate water transfer in dairy powders (Richard *et al.*, 2012; Hauser and Amamcharla, 2016;). Gas in powders consists of interstitial (between particles) and occluded (within particles) air. In the samples studied, greater quantities of both were present in high-protein powders such as MPC90 (Table 1), but flip-flop kinetic analysis of MPC90 (0.2%) indicated that only occluded air was detected by

BARDS (see Section 3.7); thus, the higher levels of occluded air in high-protein MPCs were responsible for the greater total volume of gas which was released during their rehydration (Figure 3). The volume of compressible gas generated was, as would be expected, in proportion to the mass of powder added to the water (Figure 5).

Figure 3B demonstrates that at concentrations of 0.2% gas was released much more slowly into the solvent during the rehydration of high-protein MPCs (MPC80, MPC85 and MPC90) compared to the lower protein MPCs. Gas generation in these high-protein MPCs was partially delayed by slow wetting, due to their high air content and consequent poor sinkability (Table 1) but also the high hydrophobicity indicated by the large contact angle formed between the powders and water (Crowley *et al.*, 2015). However, although wetting lasted 200 s for these powders, gas generation was still dominating over gas elimination until 500 s in the BARDS spectra of 0.2% MPC80, MPC85 and MPC90, confirming that water transfer into particles continued after wetting. For MPC80 and MPC85, Figure 3C and Table 2 show that the gas disappearance phase was intermediate among the powders and similar to MPCs which did not exhibit inhibited water transfer (MPC60, MPC70). For this reason, inhibited water transfer was not considered to strongly affect the gas disappearance behaviour in MPC60, MPC70, MPC80, MPC85; instead, the impeding influence of solubilised protein on bubble escape (Ybert and di Meaglio, 1998) was considered to define gas elimination in these systems. The more rapid gas disappearance for MPC35 and MPC50, which displayed similarly fast water transfer to MPC60 and MPC70, was likely due to the lower levels of protein available to impede bubble escape. Indeed, it was demonstrated in this study that the properties of a protein solution can influence bubble escape (Fig. 6) during the rehydration of a solute, which is an important consideration when conducting rehydration assessments using BARDS and other sound-based methods.

The rate of gas disappearance for MPC90 was the slowest of all the powders, which suggested that water transfer into powder particles was still influential during the gas disappearance phase; however, the influence of water transfer and solvent properties needed to be differentiated. Although certain physicochemical properties of a 0.2% MPC90 suspension (which had undergone complete water transfer) affected gas bubble elimination (Figure 6), slow water transfer into the powder particles was determined to be the major factor limiting gas disappearance from the solvent. The influence of the markedly slow process of water transfer into particles therefore persisted throughout the, intermediate and

late stages in the BARDS spectra for MPC90. A study of concentration-dependency, however, revealed differences between MPC80 and MPC90, which has also been observed previously for their dispersion characteristics (Crowley *et al.*, 2015). For MPC80 (gas elimination-limiting), the rate of gas disappearance was affected by concentration effects such as soluble protein, but this was not the case for MPC90 (gas generation-limiting), as the process of water transfer was not influenced by concentration (Figure 6).

Cryo-SEM micrographs indicated that the dispersion of particles on the transition from a dry powder (Figure 8) into a rehydrated solution (Figure 9) was slower and less complete for MPC90 compared to MPC35, due to the poor dispersibility of particles in high-protein MPCs (Fang *et al.*, 2011; Mimouni *et al.*, 2009; Crowley *et al.*, 2015; Li *et al.*, 2016). The cryo-SEM micrographs can be compared to the BARDS spectra in Figure 10. At 100 s of rehydration, MPC35 had a limited BARDS frequency deflection due to the quick dispersion of particles capable of releasing the minor levels of occluded air present (Table 1). As large structures capable of entrapping air were no longer present due to effective dispersion, MPC35 rapidly reached steady state before 1000 s had elapsed; conversely, water transfer into MPC90 particles was slow, and the particles themselves underwent more limited dispersion, resulting in continued air release from the particles. When particles in both MPCs had undergone significant dispersion into smaller fragments and dissolution into component molecules, neither powder exhibited any air release (~3000 s). However, at this point, the rehydration state of both powders cannot be considered equivalent, as it is clear that much larger particle structures remained in the MPC90. The MPC35 primarily consisted of particles <1 μm , which would be expected for the nanoscale proteins present in milk. On the other hand, MPC90 contained a substantial proportion of micron-sized particles, which were presumably undispersed powder particle fragments.

BARDS data indicating inhibited water transfer during the rehydration of high-protein MPCs, particularly MPC90, must be considered in the context of a growing body of evidence supporting the presence of a 'skin' of inter-linked casein micelles at the surface of high-protein MPC particles, which has been linked with the poor rehydration characteristics of these powders (McKenna, 2000; Mimouni *et al.*, 2010b; Fyfe *et al.*, 2011; Crowley *et al.*, 2016; Ji *et al.*, 2016). The results of the present study suggest that this skin of inter-packed casein micelles may act as a barrier which reduces the rate of water transfer into particles during the rehydration of high-protein MPCs. The protein:lactose ratio at the surface of the MPC particles studied here decreased significantly as the protein content of the powders

increased (Kelly *et al.*, 2015). This altered surface composition may have removed lactose as a hydrophilic channel for effective water transfer into the particle resulting in a relatively homogenous and hydrophobic particle surface (Fyfe *et al.*, 2011; Crowley *et al.*, 2015). The absence of lactose as a physical ‘spacer’ may also have promoted the tendency for proteins-protein interactions resulting in cohesive protein skin (Anema, 2006; Havea, 2006). The BARDS data and cryo-SEM micrographs in Figures 8, 9 and 10 strongly support that both water transfer and dispersibility are impaired in high-protein MPCs. This has also been found for MCCs, where a link between rapid water transfer and effective dispersion has been proposed (Richard *et al.*, 2012) and demonstrated (Bouvier *et al.*, 2013).

The nature of the relationship between water transfer and dispersion has yet to be established, although it is evident from the present study that MPCs with poor water transfer properties also have poor dispersion characteristics. One possibility is that incomplete water transfer results in regions of the particles remaining effectively ‘dry’, thereby limiting their ability to attain the molecular mobility necessary to disperse effectively. This concept is illustrated in Figure 10 with corresponding BARDS frequency profile for MPC90, which shows how the presence of dry regions near the internal air vacuole of the particle could result in the predominance of uni-directional (towards the bulk solvent) dispersion, where components in immediate contact with the solvent are released first by an erosion-like process. Transfer of water through the protein skin during rehydration could eventually expose dry regions to a second solvent-front located in the interior of the particle. The presence of these two solvent-fronts would then promote collapse of the particle through multi-directional (towards the particle interior and the bulk solvent) dispersion.

5. Conclusion

BARDS was demonstrated to be an effective method for discriminating between MPC powders with different rehydration characteristics. The BARDS experiments only required 25 mL of water and 10-50 mg of each MPC (0.04-0.20%), which minimises greatly the quantities of powder required for comparable tests. An additional advantage is that BARDS is non-invasive, as acoustic responses are derived from a non-contact microphone rather than a submerged probe. MPC35, MPC50, MPC60 and MPC70 exhibited similar water transfer properties, and differences in their BARDS spectra were primarily caused by their different air contents and the effect of increasing protein content on bubble escape. High-protein MPC powders (MPC80, MPC85 and MPC90) exhibited a characteristic BARDS response during

rehydration involving a prolonged period of gas generation to reach a maximum solvent compressibility, due mainly to inhibited water transfer into the powder particles. The period of gas generation during the rehydration of high-protein MPCs was followed by a prolonged return to steady-state equilibrium; the disappearance of gas from the solvent during this phase was influenced by the impeding effect of soluble protein on bubble escape; however, for MPC90, inhibited water transfer was still dominant during gas disappearance. The water transfer properties of high-protein MPCs were poor, but they were exceptionally poor for MPC90. BARDS is one of the few techniques currently available which facilitates the dynamic monitoring of water transfer during powder rehydration. Further BARDS studies will focus on the effect of varying solvent composition and temperature of rehydration on water transfer properties. BARDS may also be an attractive option for identifying defects in the rehydration characteristics of high-protein dairy powders caused by process- or storage-induced degradative changes.

6. Acknowledgements

The authors would like to acknowledge the Food Institutional Research Measure (FIRM) initiative of the Irish Department of Agriculture, Food and the Marine for funding the PhD project of Mr. Crowley. In addition, the authors wish to thank Enterprise Ireland and the ERDF for funding BARDS development under contracts TD-2009-0327 and TD-2011-1069. The authors would like to thank Paul Stanley and Theresa Morris, of the Centre for Electron Microscopy at the University of Birmingham, for their guidance with SEM and cryo-SEM sample preparation and imaging. Rizwan Ahmed's studentship is kindly sponsored by Alltech through the Irish Research Council Enterprise Partnership Scheme.

7. References

Agarwal, S., Beausire, R. L. W., Patel, S., and Patel, H. (2015). Innovative uses of milk protein concentrates in product development. *Journal of Food Science*, 80, S1, A23–A29.

- Anema, S. G., Pinder, D. N., Hunter, R. J., and Hemar, Y. (2006). Effects of storage temperature on the solubility of milk protein concentrate (MPC85). *Food Hydrocolloids*, 20, 386-393.
- Bouvier, J.-M., Collado, M., Gardiner, D., Scott, M., and Schuck, P. (2013). Physical and rehydration properties of milk protein concentrates: comparison of spray-dried and extrusion-porosified powders. *Dairy Science and Technology*, 93, 387-399.
- Boxenbaum, H. (1998) Pharmacokinetics Tricks and Traps: Flip-Flop Models. *Journal of Pharmacy and Pharmaceutical Sciences* 1, 3, 90-91
- Carr, A., and Golding, M. (2016). Functional milk proteins production and utilisation: casein-based ingredients, , in, *Advanced Dairy Chemistry: Volume 1: Proteins, Part B, Applied Aspects*, P. L. H. McSweeney and J. A. O'Mahony, eds., Springer, New York, pp 35-66.
- Crawford, F. S. (1982). The Hot Chocolate Effect. *American Journal of Physics*, 50, 398-404.
- Crowley, S. V., Desautel, B., Gazi, I., Kelly, A. L., Huppertz, T., and O'Mahony, J. A. (2015). Rehydration characteristics of milk protein concentrate powders. *Journal of Food Engineering*, 149, 105-113.
- Crowley, S. V., Gazi, I., Kelly, A. L., Huppertz, T., and O'Mahony, J. A. (2014a). Influence of protein concentration on the physical and flow properties of milk protein concentrate powders. *Journal of Food Engineering*, 135, 31-38.
- Crowley, S. V., Megemont, M., Gazi, I., Kelly, A. L., Huppertz, T., and O'Mahony, J. A. (2014b). Heat stability of reconstituted milk protein concentrate powders. *International Dairy Journal*, 37, 104-110
- Crowley, S. V., Jeantet, R., Schuck, P., Kelly, A. L., and O'Mahony, J. A. (2016). Rehydration and solubility characteristics of high-protein dairy powders, in, *Advanced Dairy Chemistry: Volume 1: Proteins, Part B*, P. L. H. McSweeney & J. A. O'Mahony, eds., pp 99-131, New York: Springer.
- Fang, Y., Selomulya, C., Ainsworth, S., Palmer, M., and Chen, X. D. (2011). On quantifying the dissolution behaviour of milk protein concentrate. *Food Hydrocolloids*, 25, 503-510.
- Fang, Y, Selomulya, C, Chen X. D (2008). On measurement of food powder reconstitution properties. *Drying Technology*, 26, 3-14.
- Fitzpatrick, D., Evans-Hurson, R., Fu, Y., Burke, T., Vos, B., Krüse, J., McSweeney, S., Casaubieilh, P., & Keating, J. J. (2014). Rapid Profiling of Enteric Coated Drug

- Delivery Spheres via Broadband Acoustic Resonance Dissolution Spectroscopy (BARDS). *Analyst*, 139, 1000-1106.
- Fitzpatrick, D., Evans-Hurson, R., Krüse, J., Vos, B., McSweeney, S., Casaubieilh, P., & O’Gorman, E. (2013). The relationship between dissolution, gas oversaturation and outgassing of solutions determined by Broadband Acoustic Resonance Dissolution Spectroscopy (BARDS). *Analyst*, 138, 5005-5010.
- Fitzpatrick, D., Krüse, J., Vos, B., Foley, O., Gleeson, D., O’Gorman, E., & O’Keeffe, R. (2012a). Principles and Applications of Broadband Acoustic Resonance Dissolution Spectroscopy (BARDS): A Sound Approach for the Analysis of Compounds. *Analytical Chemistry*, 84, 2202-2210.
- Fitzpatrick, D., Scanlon, E., Krüse, J., Vos, B., Evans-Hurson, R., Fitzpatrick, E., & McSweeney, S. (2012b). Blend uniformity analysis of pharmaceutical products by Broadband Acoustic Resonance Dissolution Spectroscopy (BARDS). *International Journal of Pharmaceutics*, 438(1-2), 134-139.
- Fyfe, K. N., Kravchuk, O., Le, T., Deeth, H. C., Nguyen, A. V., and Bhandari, B. (2011). Storage induced changes to high protein powders: influence on surface properties and solubility. *Journal of the Science of Food and Agriculture*, 91, 2566-2575.
- Gazi, I., and Huppertz, T. (2014). Influence of protein content and storage conditions on the solubility of caseins and whey proteins in milk protein concentrates. *International Dairy Journal*, 46, 22-30.
- Havea, P. (2006). Protein interactions in milk protein concentrate powders. *International Dairy Journal*, 16, 415-422.
- Hauser, M., and Amamcharla, J. K. (2016). Development of a method to characterize high-protein dairy powders using an ultrasonic flaw detector. *Journal of Dairy Science*, 99, 1-9.
- Ji, J., Fitzpatrick, J., Cronin, K., Maguire, P., Zhang, H., and Miao, S. (2016). Rehydration behaviours of high protein dairy powders: The influence of agglomeration on wettability, dispersibility and solubility. *Food Hydrocolloids* [in press]
doi:10.1016/j.foodhyd.2016.02.030
- Kelly, G., M., O’Mahony, J. A., Kelly, A. L., Huppertz, T., Kennedy, D., and O’Callaghan, D. (2015). Influence of protein concentration on surface composition and physico-chemical properties of spray-dried milk protein concentrate powders *International Dairy Journal*, 51, 34-40.

- 774 McKenna, A. B. (2000). Effect of processing and storage on the reconstitution properties of
 775 whole milk and ultrafiltered skim milk powders. Ph.D. thesis, Massey University,
 776 Palmerston North, New Zealand.
- 777 Mimouni, A., Deeth, H. C., Whittaker, A. K., Gidley, M. J., and Bhandari, B. R. (2009).
 778 Rehydration process of milk protein concentrate powder monitored by static light
 779 scattering. *Food Hydrocolloids*, 23, 1958-1965.
- 780 Mimouni, A., Deeth, H. C., Whittaker, A. K., Gidley, M. J., and Bhandari, B. R. (2010a).
 781 Rehydration of high-protein-containing dairy powder: slow- and fast-dissolving
 782 components and storage effects. *Dairy Science and Technology*, 90, 335-344.
- 783 Mimouni, A., Deeth, H. C., Whittaker, A. K., Gidley, M. J., and Bhandari, B. R. (2010b).
 784 Investigation of the microstructure of milk concentrate powders during rehydration:
 785 alterations during storage. *Journal of Dairy Science*, 93, 463-472.
- 786 Richard, B., Toubal, M., Le Page, J.-F., Nassar, G., Radziszewski, E., Nongaillard, B.,
 787 Debreyne, P., Schuck, P., Jeantet, R., and Delaplace, G. (2012). Ultrasound tests in a
 788 stirred vessel to evaluate the reconstitution ability of dairy powders. *Innovative Food*
 789 *Science and Emerging Technologies*, 16, 233-242.
- 790 Rowland, M. and Tozer, T.N. (1989). Clinical pharmacokinetics. Concepts and Applications
 791 (second edition). Lea & Febriger (UK) Ltd.
- 792 Sadek, C., Schuck, P., Fallourd, Y., Pradeau, N., Jeantet, R., and Le Fouéré, C. (2016).
 793 Buckling and collapse during drying of a single aqueous dispersion of casein micelle
 794 droplet. *Food Hydrocolloids*, 52, 161-166.
- 795 Schuck, P., Davenel, A., Mariette, F., Briard, V., Méjean, S., and Piot, M. (2002).
 796 Rehydration of casein powders: effects of added mineral salts and salt addition
 797 methods on water transfer. *International Dairy Journal*, 12, 51-57.
- 798 Sikand, V., Tong, P.S., Roy, S., Rodriguez-Saona, L.E., and Murray, B.A. (2011). Solubility
 799 of commercial milk protein concentrates and milk protein isolates. *Journal of Dairy*
 800 *Science*, 94, 6194-6202.
- 801 Wood, A. B. (1930). *A Textbook of Sound* (1st ed.). New York: Macmillan.
- 802 Ybert, C., and di Meglio, J.-M. (1998). Ascending air bubbles in protein solutions. *European*
 803 *Physical Journal B: Condensed Matter and Complex Systems*, 4, 313-319.

1 **Figure Legends**

2 **Figure 1.** Principal of BARDS analysis as applied to MPC rehydration: Panel 1, Schematic of
 3 the BARDS Instrument; Panel 2, Addition of MPC powder to the BARDS dissolution vessel;
 4 Panel 3, Water/Air transfer of an MPC particle during rehydration and raw BARDS spectra
 5 of the rehydration of 50 mg of MPC90 in 25 mL of deionised water at 22 °C.

6 **Figure 2.** Comparison of BARDS spectra of all MPC powders dissolved in 25 mL deionised
 7 water at 22 °C with a consistent sample concentration of 0.2% (w/v).

8 **Figure 3.** Concentration-dependence of BARDS frequency response during rehydration of
 9 MPC in deionised water at 22 °C: (A) MPC35; (B) MPC70; (C) MPC80; (D) MPC90.

10 **Figure 4.** Gas volume-time plots derived from BARDS frequency data: (A) Gas volume plots
 11 of all MPCs tested during rehydration of 50 mg MPC in 25 mL water at 22 °C; (B)
 12 Magnification of gas volume profile during the initial phase shown in (A); (C) A log plot of
 13 the gas volumes in (A), the slopes of which are used to calculate the BARDS first-order rate
 14 constants (k).

15 **Figure 5.** Gas volume plots for (A) MPC35, (B) MPC 70, (C) MPC80 and (D) MPC90, using
 16 a logarithmic scale for the gas volume.

17 **Figure 6.** Investigation of influence of solvent properties on gas disappearance: (A)
 18 Frequency-time plot of MPC dissolved in water, KCl dissolved in water or KCl dissolved in
 19 MPC90 solution; (B) log plot of gas volume data derived from (A).

20 **Figure 7.** Modelling of BARDS data using flip-flop kinetics: (A) Modelling of 0.2% MPC90
 21 data, as presented in Fig. 3A. (B) Log plot and simulation of the data in (A). (C) Modelling of
 22 0.2% MPC90 data obtained under slightly different conditions and (D) log plot and
 23 simulation of the data in (C).

24 **Figure 8.** Cryo-SEM micrographs of dry (1) MPC35, (2) MPC70 and (3) MPC90 at
 25 magnifications of (A) 500× and (B) 2500×, with scale bars of 50 and 10 µm, respectively, for
 26 the magnifications.

27 **Figure 9.** BARDS spectra of all MPCs added at 0.2% w/v and cryo-SEM micrographs of (1)
 28 MPC35 and (2) MPC90 after rehydration for (A) 100 s, (B) 1000 s, and (C) 3000 s.

29 Corresponding rehydration times in the BARDS spectra and micrographs are indicated for
30 comparison.

31 **Figure 10.** Schematic representation of protein 'skin' at the surface of a primary powder
32 particle in a high-protein MPCs and the hypothesised relationship between inhibited water
33 transfer and the poor dispersion of these particles. A BARDS profile for MPC90 is shown.

Table 1. Composition and physical properties of milk protein concentrates (MPCs). Data presented are the means of duplicate analysis, with the exception of lactose, which was the result of a single analysis.^a

Table 2. Results from kinetic analysis of log gas volume-time plots taken from BARDS measurement of different MPC powders.

Tables

Table 1. Composition and physical properties of milk protein concentrates (MPCs). Data presented are the means of duplicate analysis, with the exception of lactose, which was the result of a single analysis.^a

	Composition				Physical properties		
	Protein	Lactose	Ash	Fat	d ₅₀ ^b	Interstitial air	Occluded air
	(%, w/w)				(µm)	(ml 100 g ⁻¹)	
MPC35	35.4	49.6	8.06	0.5	35.3	98	18.1
MPC50	49.9	35.8	7.75	0.8	43.0	88	14.1
MPC60	60.8	24.5	7.74	1.5	48.9	95	21.4
MPC70	68.3	18.0	7.99	1.2	39.6	111	23.0
MPC80	79.1	6.36	7.69	1.7	27.9	206	53.7
MPC85	84.0	1.81	7.54	1.2	26.1	229	47.2
MPC90	85.9	0.37	7.59	1.6	26.8	230	46.2

^a taken from Crowley *et al.* (2014a).

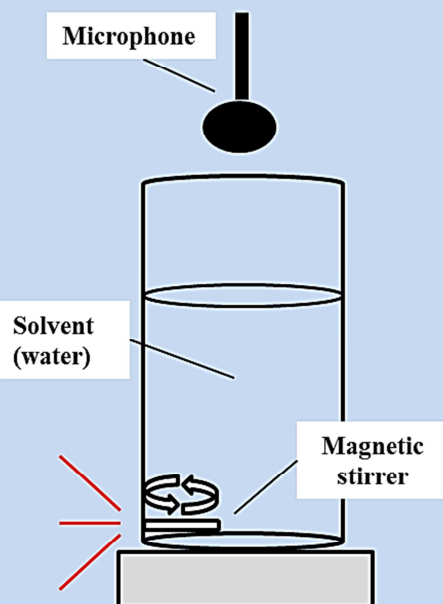
^b Particle size below which 50% of material volume exists – median.

Table 2. Results from kinetic analysis of log gas volume-time plots taken from BARDS measurement of different MPC powders.

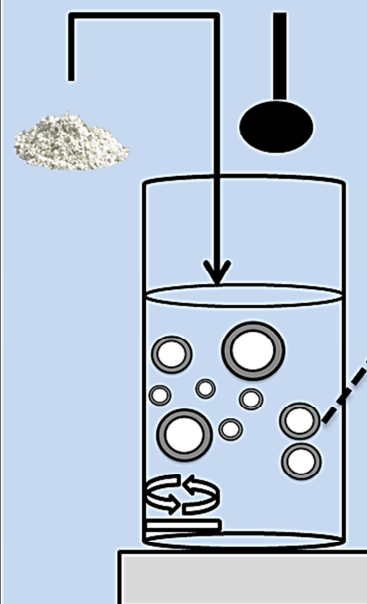
Compressible gas volume disappearance rate constant: k (s^{-1})														
Conc.	MPC35	fit	MPC50	fit	MPC60	fit	MPC70	fit	MPC80	fit	MPC85	fit	MPC90	fit
% (w/v)	k (s^{-1})	range (s)	k (s^{-1})	range (s)	k (s^{-1})	range (s)	k (s^{-1})	range (s)	k (s^{-1})	range (s)	k (s^{-1})	range (s)	k (s^{-1})	range (s)
0.2	1.0E-02	220 -500	2.5E-02	40 -160	3.7E-03	240 -1500	6.6E-03	70 - 300	3.4E-03	500 -2000	3.88E-03	800 - 1800	1.9E-03	500 -2500
			9.5E-03	160 - 300			3.7E-03	400 - 1400						
0.16	1.0E-02	220 -500					1.3E-02	120 - 200					1.8E-03	400 -2700
							7.9E-03	220 - 500						
0.12	1.0E-02	220 -500					1.3E-02	120 - 200	4.3E-03	400 -1300			1.8E-03	400 -2100
							7.9E-03	220 - 500						
0.08	4.4E-02	60 -90					1.6E-02	120 - 220	4.9E-03	400 -1200			2.1E-03	700 -2400
	1.0E-02	120 -260					7.0E-03	240 - 500						
0.04	5.3E-02	40 -90					1.1E-02	60 - 180	6.7E-03	300 -600			2.8E-03	600 -1500
							7.1E-03	260 - 400	9.8E-03	100 -220				

Use of BARDS to monitor water transfer phenomena in MPC powders over time

1. Contact between a magnetic stirring bar and the vessel wall induces acoustic resonances which are detected by a microphone located above the vessel.



2. Addition of powder to the solvent introduces particles which release air as they are penetrated by water. Alterations to the acoustic resonance profile are measured over time.



3. Release of air changes the compressibility of the solvent, which results in a frequency profile that undergoes time-dependant changes, and is indicative of water transfer.

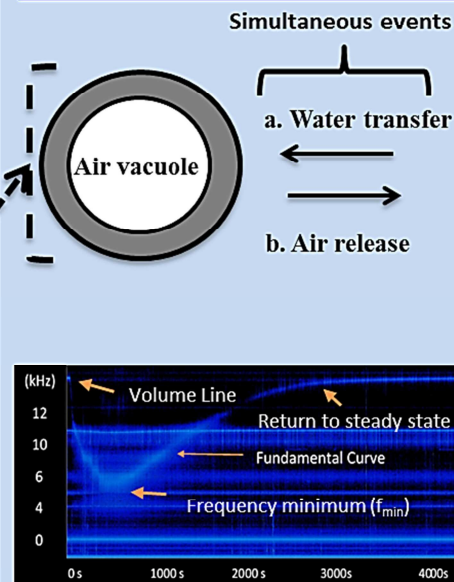
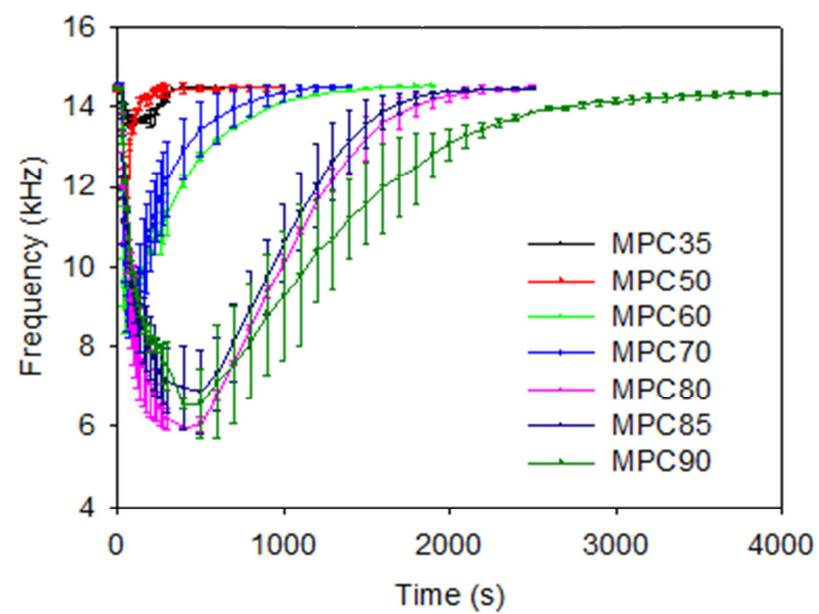
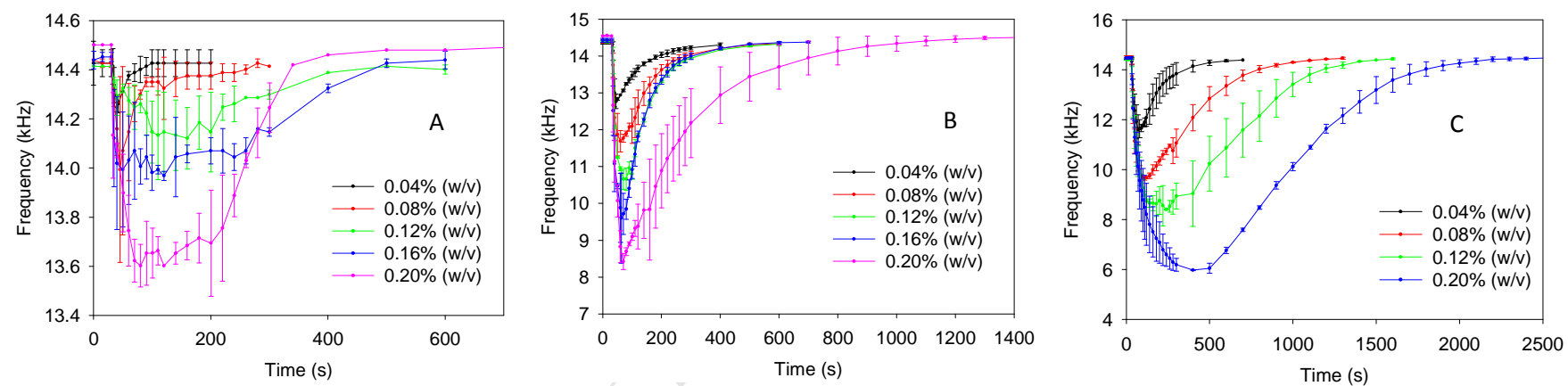


Figure 1.**Figure 2:**

**Figure 3**

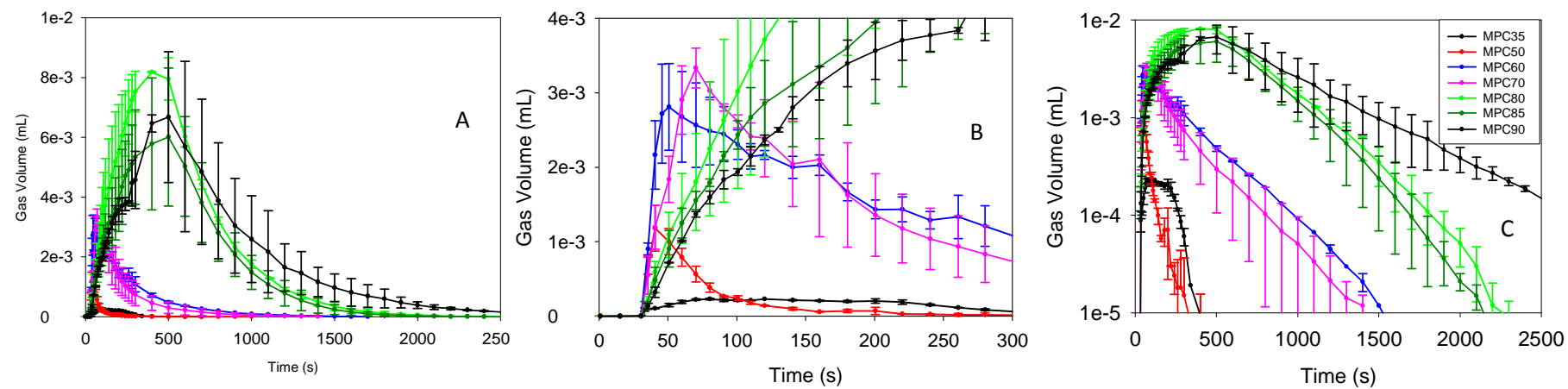


Figure 4.

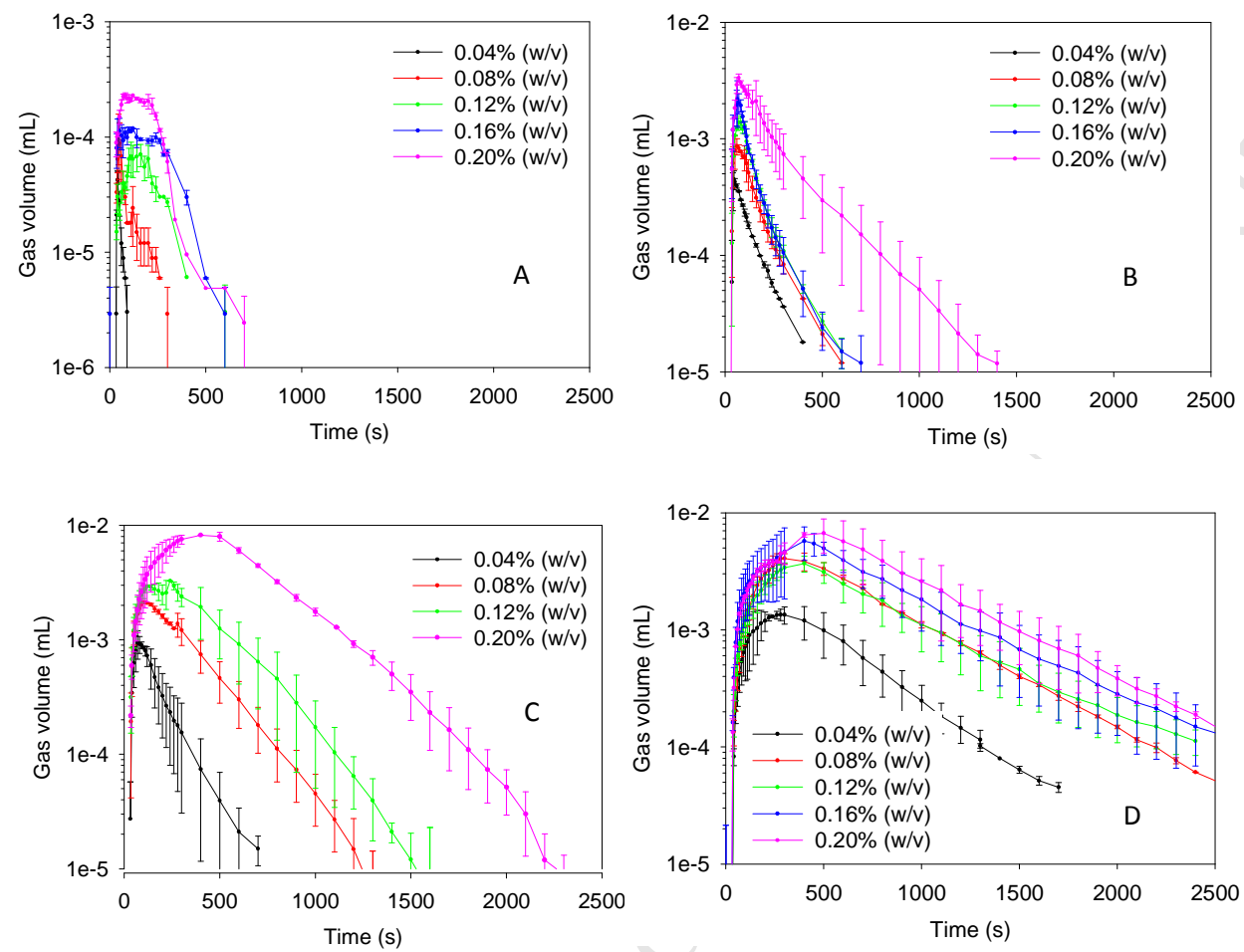


Figure 5:

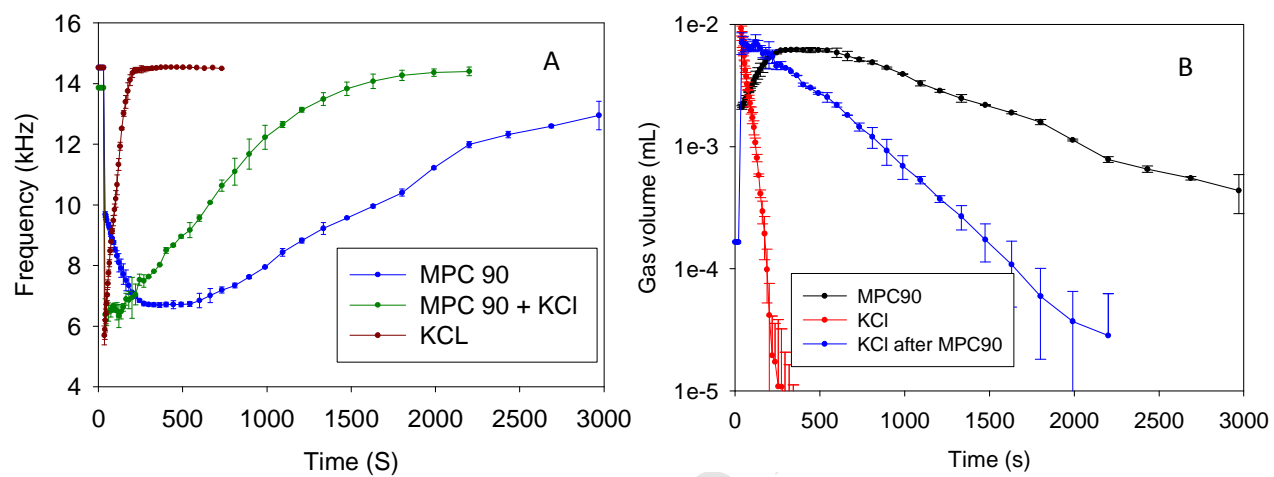
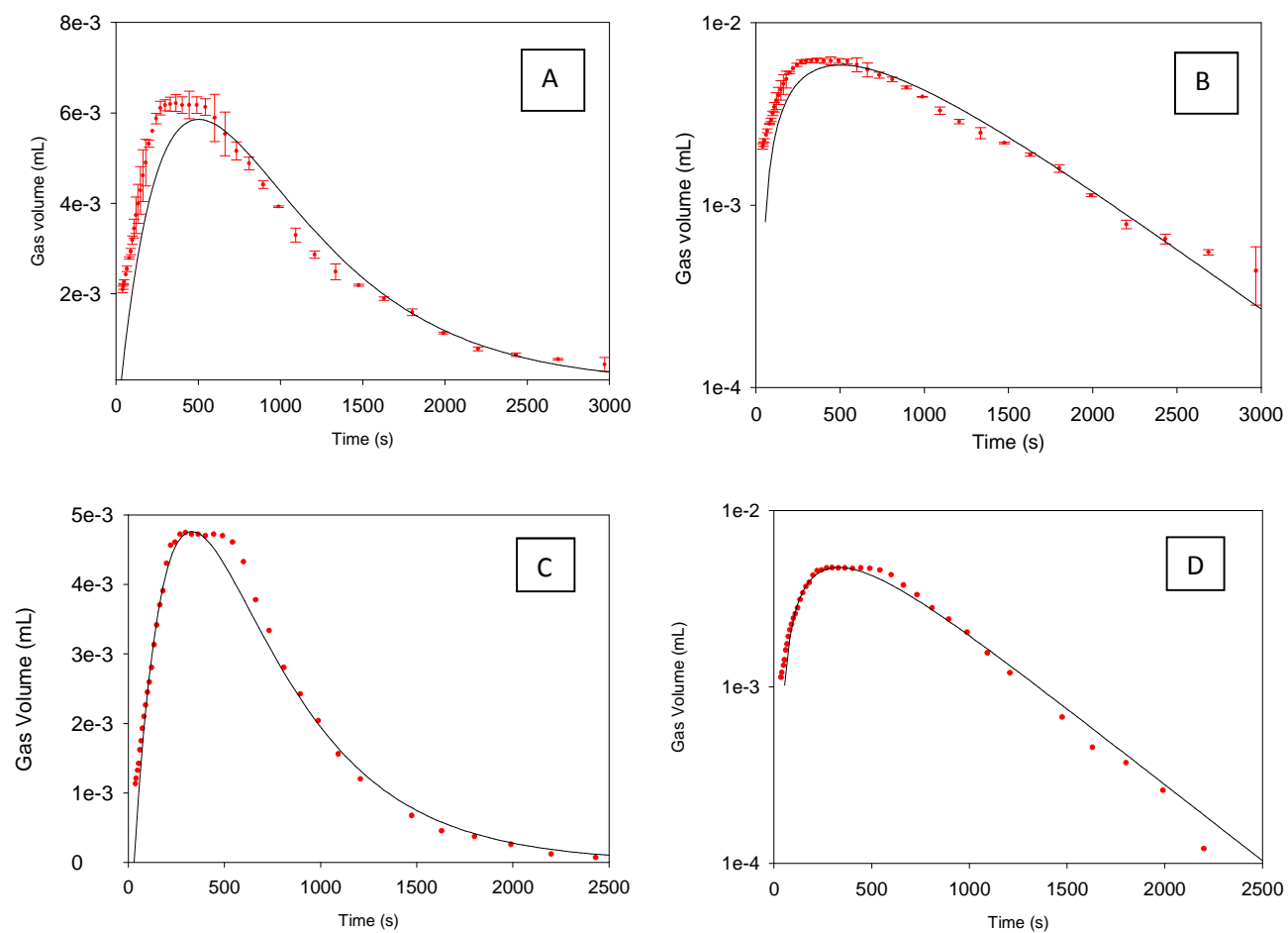


Figure 6.

**Figure 7.**

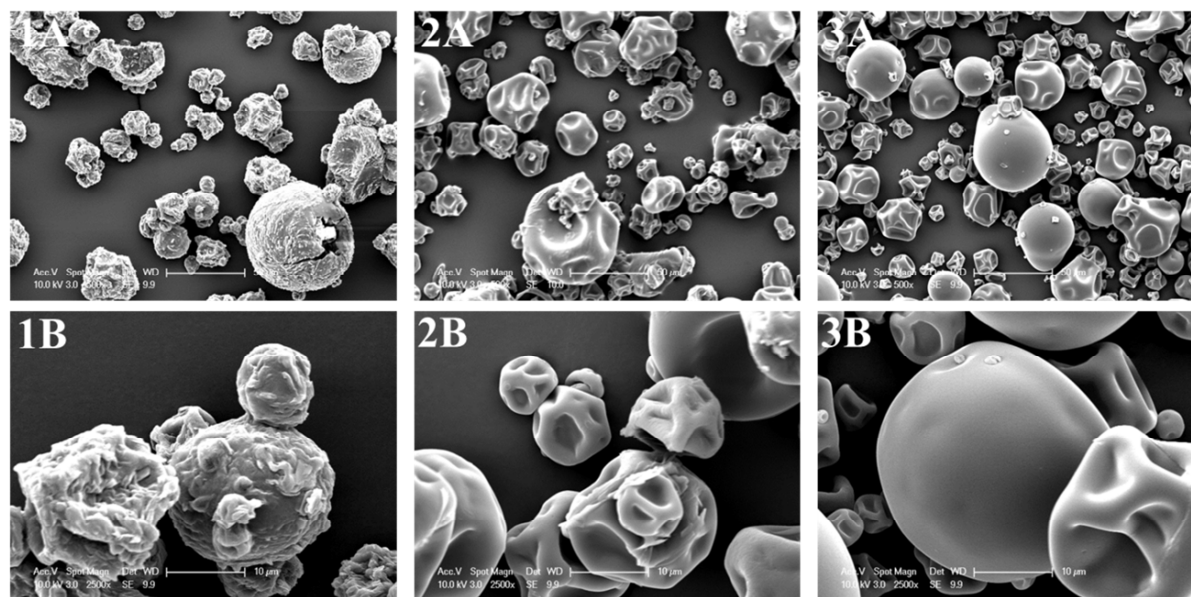
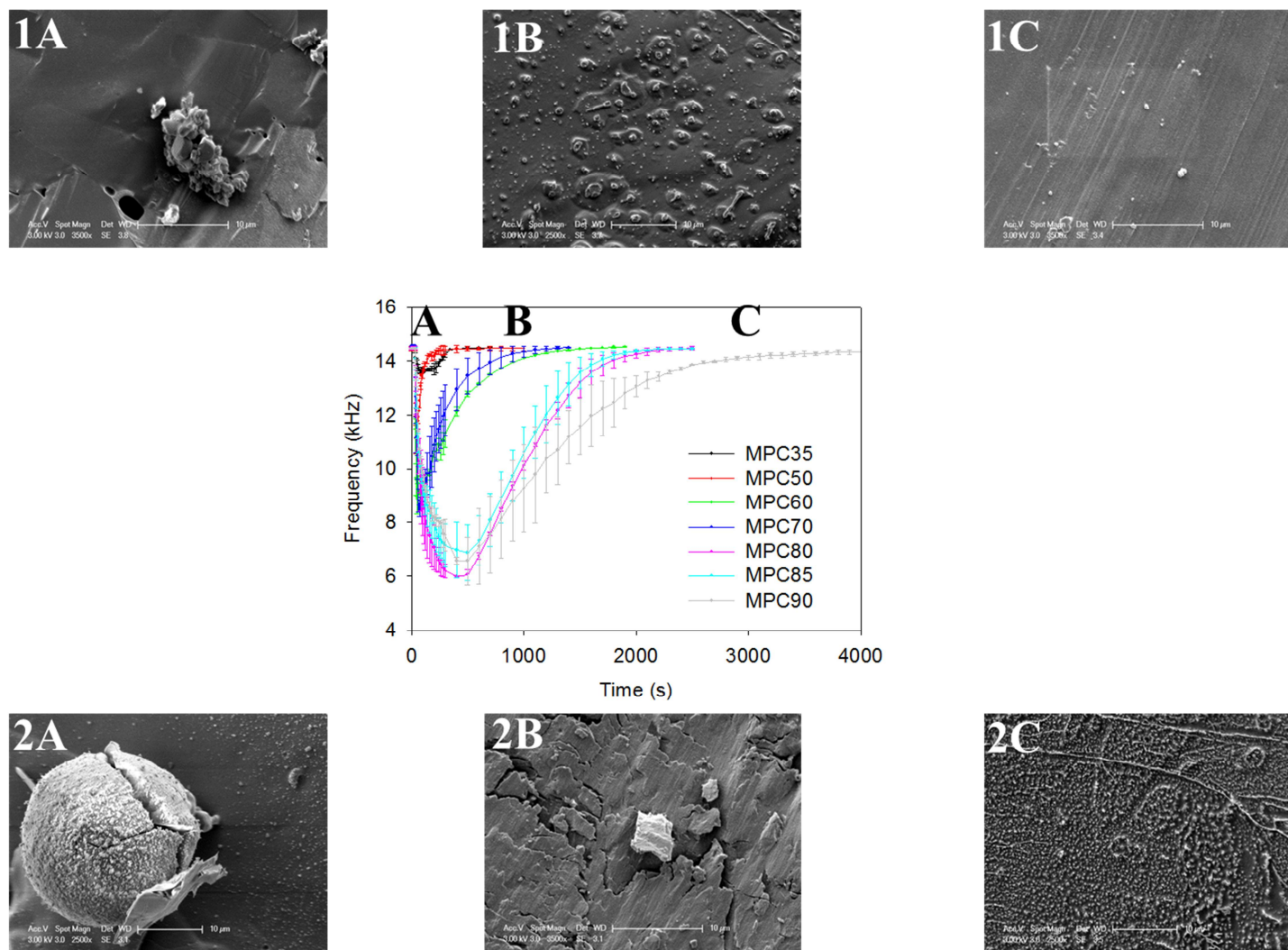


Figure 8.

**Figure 9.**

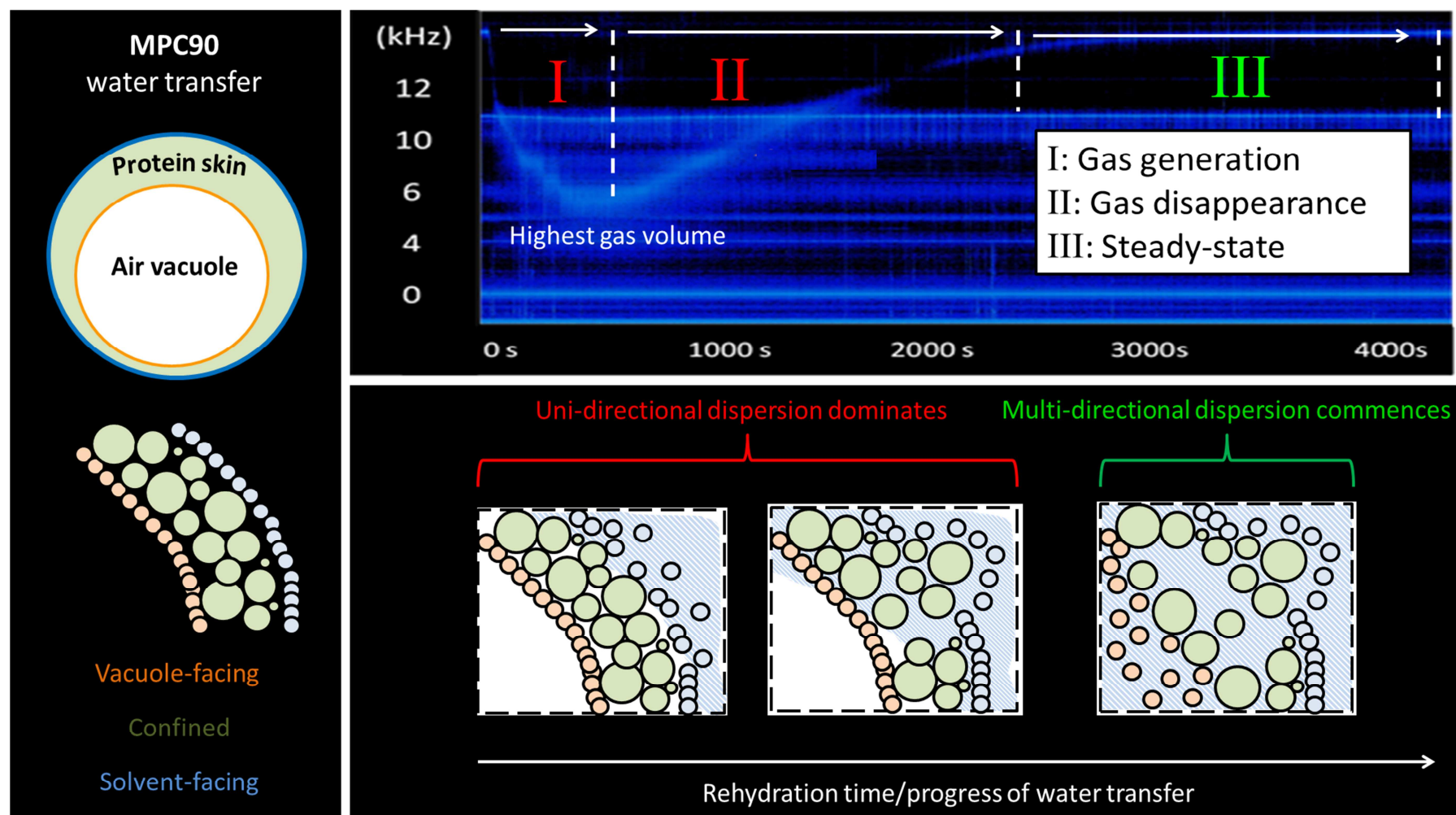


Figure 10.

Highlights

- BARDS measured changes in gas volume during MPC rehydration
- Gas generation/escape rates decreased with increasing protein content
- Occluded air from particles constituted the gas generated
- BARDS indicates water transfer was markedly inhibited in MPC90
- The hydration process of high MPC samples have been quantitatively modelled.
- Cryo-SEM confirmed slow water transfer/poor dispersion link